



**HAL**  
open science

## Effects on surface atmospheric photo-oxidants over Greece during the total solar eclipse event of 29 March 2006

P. Zanis, E. Katragkou, M. Kanakidou, B. Psiloglou, S. Karathanasis, M. Vrekoussis, E. Gerasopoulos, I. Lysaridis, K. Markakis, A. Poupkou, et al.

► **To cite this version:**

P. Zanis, E. Katragkou, M. Kanakidou, B. Psiloglou, S. Karathanasis, et al.. Effects on surface atmospheric photo-oxidants over Greece during the total solar eclipse event of 29 March 2006. *Atmospheric Chemistry and Physics Discussions*, 2007, 7 (4), pp.11399-11428. hal-00303024

**HAL Id: hal-00303024**

**<https://hal.science/hal-00303024>**

Submitted on 18 Jun 2008

**HAL** is a multi-disciplinary open access archive for the deposit and dissemination of scientific research documents, whether they are published or not. The documents may come from teaching and research institutions in France or abroad, or from public or private research centers.

L'archive ouverte pluridisciplinaire **HAL**, est destinée au dépôt et à la diffusion de documents scientifiques de niveau recherche, publiés ou non, émanant des établissements d'enseignement et de recherche français ou étrangers, des laboratoires publics ou privés.

# Effects on surface atmospheric photo-oxidants over Greece during the total solar eclipse event of 29 March 2006

P. Zanis<sup>1</sup>, E. Katragkou<sup>2</sup>, M. Kanakidou<sup>3</sup>, B. Psiloglou<sup>4</sup>, S. Karathanasis<sup>5</sup>,  
M. Vrekoussis<sup>3,\*</sup>, E. Gerasopoulos<sup>4</sup>, I. Lysaridis<sup>2</sup>, K. Markakis<sup>2</sup>, A. Poupkou<sup>2</sup>,  
V. Amiridis<sup>4</sup>, D. Melas<sup>2</sup>, N. Mihalopoulos<sup>3</sup>, and C. Zerefos<sup>4</sup>

<sup>1</sup>Department of Meteorology and Climatology, Aristotle University of Thessaloniki, Greece

<sup>2</sup>Laboratory of Atmospheric Physics, Aristotle University of Thessaloniki, Greece

<sup>3</sup>Environmental Chemical Processes Laboratory, Department of Chemistry, University of Crete, Greece

<sup>4</sup>National Observatory of Athens, Athens, Greece

<sup>5</sup>Region of Central Macedonia, Thessaloniki, Greece

\* now at: Institute of Environmental Physics and Remote Sensing IUP/IFE, University of Bremen, Germany

Received: 20 July 2007 – Accepted: 20 July 2007 – Published: 2 August 2007

Correspondence to: P. Zanis (zanis@auth.gr)

**Eclipse effects on  
surface atmospheric  
photooxidants**

P. Zanis et al.

Title Page

Abstract

Introduction

Conclusions

References

Tables

Figures

◀

▶

◀

▶

Back

Close

Full Screen / Esc

Printer-friendly Version

Interactive Discussion

## Abstract

This study investigates the effects of the total solar eclipse of 29 March 2006 on surface air-quality levels over Greece based on observations at a number of sites in conjunction with chemical box modelling and 3-D air-quality modelling. Emphasis is given on surface ozone and other photooxidants at four Greek sites Kastelorizo, Finokalia (Crete), Pallini (Athens) and Thessaloniki, which are located at gradually increasing distances from the path of the eclipse totality and are characterized by different air pollution levels. The eclipse offered the opportunity to test our understanding of air pollution build-up and the response of the gas-phase chemistry of photo-oxidants during a photolytical perturbation using both a photochemical box model and a regional air-quality offline model based on the modeling system WRF/CAMx. At the relatively unpolluted sites of Kastelorizo and Finokalia no clear impact of the solar eclipse on surface  $O_3$ ,  $NO_2$  and  $NO$  concentrations can be deduced from the observations and model simulations as the calculated changes in net ozone production rates between eclipse and non eclipse conditions are rather small compared to the ozone variability and hence the solar eclipse effects on ozone can be easily masked by transport. At the polluted sites of Thessaloniki and Pallini, the solar eclipse effects on  $O_3$ ,  $NO_2$  and  $NO$  concentrations are clearly revealed from both the measurements and 3-D air-quality modeling with the net effect being a decrease in  $O_3$  and  $NO$  and an increase in  $NO_2$  as  $NO_2$  formed from the reaction of  $O_3$  with  $NO$  while at the same time  $NO_2$  is not efficiently photolysed. It is evident from the 3-D air quality modeling over Greece that the maximum effects of the eclipse on  $O_3$ ,  $NO_2$  and  $NO$  are reflected at the large urban agglomerations of Athens, and Thessaloniki where the maximum of the emissions occur.

## 1 Introduction

The effects of a solar eclipse on total ozone column and stratospheric ozone have been reported by several authors (Zerefos et al., 2000, and references therein). However,

ACPD

7, 11399–11428, 2007

## Eclipse effects on surface atmospheric photooxidants

P. Zanis et al.

Title Page

Abstract

Introduction

Conclusions

References

Tables

Figures

◀

▶

◀

▶

Back

Close

Full Screen / Esc

Printer-friendly Version

Interactive Discussion

EGU

there is only a limited number of studies concerning the solar eclipse induced effects on tropospheric ozone and other photooxidants (Srivastava et al., 1982; Fabian et al., 2000; Zanis et al., 2001; Zerefos et al., 2001).

During a solar eclipse solar radiation changes may affect tropospheric ozone in several ways and timescales. Tropospheric ozone concentrations maybe directly affected by the  $JO^1D$  and  $JNO_2$  photolysis rate constants changes and indirectly by the  $NO_x$  and  $HO_x$  budget modifications. Both change the relative strength of sources and sinks of tropospheric  $O_3$ . A fast response of tropospheric ozone to solar eclipse stems from the decrease of  $JNO_2$  which induces a perturbation from the photostationary steady state of  $O_3$ ,  $NO$  and  $NO_2$  in Reactions (R1), (R2) and (R3):



As a direct consequence the primary pollutant  $NO$  destroys  $O_3$  through the titration Reaction (R3) without  $O_3$  being resumed through the  $NO_2$  photolysis (R1). This fast ozone response to solar eclipse can be clearly identified in relatively polluted sites such as urban and suburban sites.

A slower response of tropospheric ozone to solar eclipse can result from changes in the UV-B radiation which affect the photolysis rate constant  $JO^1D$  that photodissociates ozone in the near UV. Changes in UV-B induce changes in the direct ozone loss rate via Reaction (R4), of the production rate of the hydroxyl radical  $OH$  (in the presence of water vapor) via reaction (R5) and of the hydroperoxy radicals via Reactions (R6) and (R7):



## Eclipse effects on surface atmospheric photooxidants

P. Zanis et al.

Title Page

Abstract

Introduction

Conclusions

References

Tables

Figures

◀

▶

◀

▶

Back

Close

Full Screen / Esc

Printer-friendly Version

Interactive Discussion



In turn, changes in the OH and HO<sub>2</sub> concentrations induce changes in the rates of ozone loss pathways via Reactions (R8) and (R9):



and in the ozone production pathway via reaction (R10) when NO is present :



10 The photolysis of other species which are secondary sources of radicals such as HCHO ( $\lambda < 330 \text{ nm}$ ) or CH<sub>3</sub>CHO ( $\lambda < 330 \text{ nm}$ ) via radical formation can also affect the surface ozone concentrations. Therefore, surface ozone is expected to be susceptible to solar radiation changes observed during eclipse events.

15 Zanis et al. (2001) showed that during the eclipse of 11 August 1999 the surface ozone displayed a decrease of around 10–15 ppbv at the urban site of Thessaloniki, Greece (90% sun disk obscuration) while at the rural elevated site of Hohenpeisenberg, Germany (99.4% sun disk obscuration) the actual surface ozone data did not show any clear eclipse effect. During the 11 August 1999 eclipse event, Mavrakis et al. (2004) found ozone responses to the eclipse over the greater Athens area that varied in terms of timing and intensity as a function of the local emissions, the local topography and the distance from the seashore. Photochemical box model simulations for Freising-Weihenstephan, Germany for the same eclipse event suggested a 4 ppb reduction in the net O<sub>3</sub> production until the end of the eclipse. Both measurements and model simulations showed that the partitioning of NO<sub>x</sub> between NO and NO<sub>2</sub> was determined almost exclusively by the variations in JNO<sub>2</sub> (Fabian et al., 2001).

25 The present work investigates the chemical effects of the solar eclipse of 29 March 2006 on surface ozone and other photo-oxidants over Greece. Taking advantage that

## Eclipse effects on surface atmospheric photooxidants

P. Zanis et al.

Title Page

Abstract

Introduction

Conclusions

References

Tables

Figures

◀

▶

◀

▶

Back

Close

Full Screen / Esc

Printer-friendly Version

Interactive Discussion

part of southeastern Greece experienced the totality of solar eclipse, combined measurements of air quality and meteorological parameters were organized at sites located at different distances from the eclipse path. The different solar obscuration at each site combined with a variety of air quality measurements has enabled a thorough representation and investigation of the response of photochemistry to an abrupt photolytical perturbation.

## 2 Data and methods

### 2.1 Description of measurements

The eclipse effects during the 29 March 2006 on the biosphere and on various atmospheric layers have been investigated in the frame of a field experiment over Greece. Details about the organization of the experimental campaigns, the measurement sites, eclipse path maps as well as information about the eclipse circumstances for each location are given in an overview paper by Gerasopoulos et al. (2007)<sup>1</sup>. The measurements used in this study were carried out at two urban sites, Pallini (greater Athens area) and Thessaloniki and at two marine rural sites, Finokalia (Crete) and Kastelorizo Island.

The Institute for Environmental Research and Sustainable Development (IERSD) of the National Observatory of Athens (NOA), contacted measurements of gas-phase air pollutants using their automobile station in the framework of the eclipse campaign at Kastelorizo Island. This air quality monitoring includes measurements of (i) ozone (O<sub>3</sub>), (ii) nitrous oxides (NO and NO<sub>2</sub>), and (iii) carbon monoxide (CO), with the use of HORIBA Air Pollution Monitoring Systems (AP-360 series). All air quality analyzers were carefully calibrated on site using specific gases of known concentration. In addition, various meteorological observations were carried out from a fully automated

<sup>1</sup>Gerasopoulos, E., Zerefos, C. S., Tsagouri, I., et al.: The Total Solar Eclipse of March 2006: Overview, Atmos. Chem. Phys. Discuss., submitted, 2007.

## Eclipse effects on surface atmospheric photooxidants

P. Zanis et al.

Title Page

Abstract

Introduction

Conclusions

References

Tables

Figures

◀

▶

◀

▶

Back

Close

Full Screen / Esc

Printer-friendly Version

Interactive Discussion

**Eclipse effects on  
surface atmospheric  
photooxidants**

P. Zanis et al.

Title Page

Abstract

Introduction

Conclusions

References

Tables

Figures

◀

▶

◀

▶

Back

Close

Full Screen / Esc

Printer-friendly Version

Interactive Discussion

meteorological station: (i) air temperature and relative humidity, (ii) atmospheric pressure, (iii) wind speed and direction (6 meters height), (iv) u, v and w wind components using an ultra-sound sonic anemometer, (v) total solar radiation on a horizontal surface, and (vi) direct solar radiation. All parameters were recorded with 1 min time resolution, except for the ultra-sound sonic anemometer measuring at a frequency of 21 Hz.

The monitoring station of the University of Crete at Finokalia, Lasithi, Crete is located 70 km eastward of Heraklion (about 140 thousand inhabitants) and 25 km west of Agios Nikolaos (about 20 thousand inhabitants), the nearest big cities in the area. These cities do not have any noticeable influence on the site due to the prevailing north winds. The station is located on the north coast of Crete exposed to the sea from 270°–90° (W–E). An automated meteorological station enables measurements of air temperature, relative humidity, wind speed and direction and total solar radiation. The photodissociation rates of NO<sub>2</sub> (JNO<sub>2</sub>) and O<sub>3</sub> to O<sup>1</sup>D (JO<sup>1</sup>D) as well as Radon-222 (<sup>222</sup>Rn), O<sub>3</sub>, NO, NO<sub>2</sub>, PM<sub>10</sub>, and other chemical tracers are also monitored and registered every 5 min (2 h for Radon), (Mihalopoulos et al., 1997; Gerasopoulos et al., 2005, 2006). Details about the station and the instrumentation are presented at <http://finokalia.chemistry.uoc.gr/>.

The Air Quality Monitoring Network of Athens International Airport (AIA) operates since October 1998 and consists of five permanent and one mobile monitoring stations. The permanent stations are installed in the Municipalities of Glyka Nera, Koropi, Markopoulo, Pallini and Spata while the mobile station is currently located at the airport premises. A wide range of pollutants is monitored using HORIBA Air Pollution Monitoring Systems (AP-360CE) including: nitrogen oxides (NO and NO<sub>2</sub>), sulphur dioxide (SO<sub>2</sub>), carbon monoxide (CO), ozone (O<sub>3</sub>), particulate matter (PM<sub>10</sub>), hydrocarbons (HCs) and benzene-toluene-xylene (BTX). The meteorological parameters measured include: wind speed and direction, air temperature, relative humidity, rainfall, solar radiation and atmospheric pressure.

In the Greater Area of Thessaloniki air quality measurements are carried out regularly since 2001 by the Region of Central Macedonia (RCM). This monitoring network

consists of eight fixed monitoring stations equipped with instruments that measure ambient levels of gaseous ( $\text{SO}_2$ ,  $\text{NO}_2$ ,  $\text{NO}$ ,  $\text{CO}$ ,  $\text{O}_3$ ) and particulate matter ( $\text{PM}_{10}$  and TSP) air pollutants using a HORIBA Air Pollution Monitoring Systems (AP-360 series). Most of the stations also collect meteorological data (wind direction, horizontal wind speed, ambient temperature and humidity). In this study we used the data collected at the air quality measurement station situated at the roof of the Physics Department of Aristotle University of Thessaloniki (AUTH). During the day of the eclipse event, the air quality ( $\text{NO}$ ,  $\text{NO}_2$  and  $\text{O}_3$ ) and meteorological (wind speed, wind direction, air temperature and relative humidity) measurements were recorded with 1 minute time resolution.

## 2.2 Box modelling

The impact of the observed changes in meteorological and chemical parameters during the eclipse on the oxidant levels has been studied with a chemical box model (ECPL box model; Poisson et al., 2001; Tsigaridis and Kanakidou, 2002; Vrekoussis et al., 2004). The commercially available software FACSIMILE (Curtis and Sweetenham, 1988), which uses automatic time step selection and error control appropriate to solve stiff equations like the system of non linear chemical reactions occurring in the troposphere, was used to solve the differential equations with a high accuracy required for chemistry studies. The chemistry scheme is a condensed chemical mechanism (about 300 chemical reactions and 140 chemical species). It is able to simulate boundary layer photochemistry of ozone, water vapour, nitrogen oxides, carbon monoxide and volatile organics as well as the chemistry of sulphur. In addition to background  $\text{O}_3/\text{NO}_x/\text{OH}/\text{CO}$  and  $\text{CH}_4$  chemistry, it also takes into account the oxidation chemistry of  $\text{C}_1\text{-C}_5$  hydrocarbons including isoprene (Tsigaridis and Kanakidou 2002; Vrekoussis et al., 2004; 2006) and biogenic sulphur oxidation mechanisms (Sciare et al., 2000). Oxidation of volatile organic compounds (VOC) by all three major oxidants ( $\text{O}_3$ ,  $\text{OH}$  and  $\text{NO}_3$ ) is considered when applicable. Heterogeneous reactions of peroxy and nitrate radicals are taken into account as explained by Tsigaridis and Kanakidou (2002) and Vrekoussis et al. (2004).

## Eclipse effects on surface atmospheric photooxidants

P. Zanis et al.

Title Page

Abstract

Introduction

Conclusions

References

Tables

Figures

◀

▶

◀

▶

Back

Close

Full Screen / Esc

Printer-friendly Version

Interactive Discussion

---

**Eclipse effects on  
surface atmospheric  
photooxidants**P. Zanis et al.

---

[Title Page](#)[Abstract](#)[Introduction](#)[Conclusions](#)[References](#)[Tables](#)[Figures](#)[◀](#)[▶](#)[◀](#)[▶](#)[Back](#)[Close](#)[Full Screen / Esc](#)[Printer-friendly Version](#)[Interactive Discussion](#)

Chemistry box model simulations have been performed over a 3-day period around the eclipse occurrence over Finokalia. The first day of the simulation was used as spin up time. Observed meteorology, photodissociation rates of  $\text{NO}_2$  and  $\text{O}_3$  ( $\text{JNO}_2$  and  $\text{JO}^1\text{D}$ ),  $\text{NO}$ ,  $\text{NO}_2$  and  $\text{O}_3$  levels have been used as input to the model every 5 min.

5 Reaction rates driven by meteorological conditions are calculated online. The model has been applied to calculate the free radical levels in the marine boundary layer and evaluate their response to the eclipse. Simulations have been performed both by considering and by neglecting the perturbation of photodissociation rates caused by the solar eclipse.

10 Similar simulations have been also performed for the other observational sites, Kastelorizo, Pallini (Athens) and Thessaloniki for the day of the eclipse.

### 2.3 Regional Air-quality modeling

The regional air quality model simulations have been performed with the Comprehensive Air quality Model (CAMx version 4.40). CAMx ran with coarse grid spacing over Greece in a spatial resolution of  $10 \times 10$  km and four fine nests with higher resolution ( $2 \times 2$  km) over the Greater Athens and Thessaloniki areas, Kastelorizo and Finokalia. The domain's vertical profile contains 15 layers of varying thickness. Layer 1 is 22 m deep, layer 2 extends between 22 and 50 m and subsequent layer depths increase with height. The uppermost layer is 1.5 km thick and extends to about 8 km.

20 The meteorological fields have been derived from the Weather Research and Forecasting (WRF version 2.1.2, January 2006) Model developed at the National Center for Atmospheric Research, operated by the University Corporation for Atmospheric Research. WRF has been modified accordingly to reproduce the event of eclipse (Founda et al., this issue). The first model domain covers the Balkan area ( $55 \times 55$  grid boxes with  $30 \times 30$  km resolution), the second domain covers Greece (nested domain with  $121 \times 121$  grid boxes and  $10 \times 10$  km resolution). The four domains with finer resolution ( $2 \times 2$  km) cover the measuring sites (Athens, Thessaloniki, Kastelorizo, Finokalia). In the vertical WRF model 31 layers between surface and 18.5 km were considered.

## Eclipse effects on surface atmospheric photooxidants

P. Zanis et al.

Title Page

Abstract

Introduction

Conclusions

References

Tables

Figures

⏪

⏩

◀

▶

Back

Close

Full Screen / Esc

Printer-friendly Version

Interactive Discussion

Anthropogenic and biogenic gridded emissions have been compiled for a coarse master domain covering Greece (98×108 cells, 10×10 km) and for the four nested grids with finer resolution (2×2 km). Emission data for gaseous pollutants (NMVOC, NO<sub>x</sub>, CO, SO<sub>2</sub>, NH<sub>3</sub>) and particulate matter (PM<sub>10</sub>) were estimated for different anthropogenic emission sectors such as transport, power plants, the industrial and central heating sectors. Anthropogenic emissions of the neighbouring countries (Albania, Bulgaria and Turkey) have been taken from the EMEP emission database. Diurnal biogenic emissions over Greece and neighbouring countries have been calculated for every month of the year following the EMEP/CORINAIR methodology (Poupkou et al., 2004). All emissions are injected in the first model layer of 22 m height.

Three days of simulation are regarded as “spin-up” time (26–28 March 2006) in order to eliminate the effect of initial conditions. Initial and boundary conditions corresponded to concentrations of clean air. The chemistry mechanism invoked is Carbon Bond version 4 (CB4). This mechanism includes 117 reactions – 11 of which are photolytic – and up to 67 species (37 gasses, 12 radicals and up to 18 particulates). Photolysis rates were derived for each grid cell assuming clear sky conditions as a function of five parameters: solar zenith angle, altitude, total ozone column, surface albedo, and atmospheric turbidity. The rates were taken from a large lookup table that spans the range of conditions for each of the five dimensions. This table has been developed using the TUV photolysis pre-processor following the discrete ordinates method (Madronich, 1993).

Photolysis rates have been modified for the eclipse event (09:30–12:00 UTC) by multiplication of the clear-sky photolysis rates  $J_{\text{clear}}$  with a factor per which is space- and time-dependent to simulate the differences in sun disk coverage. The presence of clouds modifies further  $J_{\text{clear}}$  according to the equation:

$$J = \text{per}(x, y, t) * [1 + F_c(A_c - 1)] * J_{\text{clear}} \quad (1)$$

where  $F_c$  is the cloud cover fraction and  $A_c$  is the vertical cloud attenuation factor, calculated separately for above and within/below clouds.

In order to analyse the photochemical model performance the Process Analysis (PA) tool has been invoked. The PA tool, implemented in CAMx, allows for a better understanding of the complex interactions in different processes and simulation results within the context of model formulation (CAMx User's Guide, 2006). Besides the standard gaseous species concentrations involved in tropospheric chemistry ( $\text{NO}_x$ ,  $\text{O}_3$  and VOCs) PA allows retrieval of information on parameters calculated by CAMx, like  $\text{O}_3$  production, photolysis rates and radical concentrations.

### 3 Results

#### 3.1 Measurements

The time series of measured  $\text{O}_3$ ,  $\text{NO}_2$  and  $\text{NO}$  and solar radiation for the four different sites during the day of eclipse are illustrated in Fig. 1 while the average concentrations of the chemical constituents during the time window of the eclipse from 09:30 to 12:00 UTC are shown in Table 1. Based on the  $\text{NO}_x$  levels at these four sites the maritime stations of Finokalia and Kastelorizo can be considered as relatively unpolluted to semi-polluted sites while the suburban/urban stations of Pallini (Athens) and Thessaloniki are polluted sites. At Kastelorizo (Fig. 1a) no major signal of solar eclipse on surface  $\text{O}_3$ ,  $\text{NO}_2$  and  $\text{NO}$  concentrations can be deduced from the observations. The only striking features are the two pollution plumes with peak concentrations of  $\text{NO}_x$  (about 90 and 15 ppbv for  $\text{NO}_2$  and  $\text{NO}$ , respectively) and the subsequent lower concentrations of  $\text{O}_3$  prior and just after the beginning of the solar eclipse. Similarly at Finokalia (Fig. 1b) no drastic changes are seen on  $\text{O}_3$ ,  $\text{NO}_2$  and  $\text{NO}$  concentrations due to the solar eclipse. However, around the maximum of the solar eclipse when surface radiation was almost extinguished at the two relatively clean sites, a decline of ozone of about 9 ppbv is observed within a ten minutes time window that is simultaneously seen at the two sites and can be partially associated with solar eclipse effects. Since transport effects can also cause such changes, chemical box modelling and regional

## Eclipse effects on surface atmospheric photooxidants

P. Zanis et al.

Title Page

Abstract

Introduction

Conclusions

References

Tables

Figures

◀

▶

◀

▶

Back

Close

Full Screen / Esc

Printer-friendly Version

Interactive Discussion

air-quality modelling have been used in order to unravel the solar eclipse contribution.

The solar eclipse effects on  $O_3$ ,  $NO_2$  and  $NO$  concentrations are more clearly marked on the measurements at Pallini station (Fig. 1c).  $O_3$  and  $NO$  concentrations show a gradual decrease from the first contact until the maximum coverage, while during the second phase ozone gradually increases reaching its prior to the eclipse levels. An opposite pattern is seen on the  $NO_2$  concentrations as the  $NO_2$  builds up during the eclipse. The  $O_3$ ,  $NO_2$  and  $NO$  measurements at Thessaloniki show similar behaviour with Pallini but with higher variability. The ozone decline at Thessaloniki during the eclipse is between 5 and 10 ppbv while  $NO$  values drop below the detection limit of the instrument during the maximum coverage of the solar disk. The differences in  $O_3$ ,  $NO_2$  and  $NO$  concentrations between their averaged values in the time window of maximum total solar obscuration (10:30–11:00 UTC) and their averaged values from both the time windows before and after the eclipse (09:30–10:00 UTC and 11:30–12:00 UTC) reveal  $O_3$  decrease by  $-8$  and  $-4$  ppbv,  $NO$  decrease by  $-1$  and  $-2$  ppbv and  $NO_2$  increase by 2, and 6 ppbv for Thessaloniki and Pallini, respectively (see Table 3).

The similar behaviour of  $O_3$ ,  $NO_2$  and  $NO$  concentrations at the two polluted sites, Pallini and Thessaloniki, can be attributed to deviation from the photostationary state of  $O_3$ ,  $NO$  and  $NO_2$  during the eclipse, with  $NO_2$  formed from the reaction of  $O_3$  with  $NO$  and not efficiently photolysed. The net effect is a decrease in  $O_3$  and  $NO$  while  $NO_2$  is accumulated. Chemical box modelling and regional air-quality modelling have been used to quantify the solar eclipse effect on photochemistry at these four Greek sites, the two relatively unpolluted and the two polluted while the observations have been used as model input or for model evaluation.

### 3.2 Box model results

Driven by the observed  $JNO_2$  and  $JO^1D$  variations during the eclipse period, the box model simulates a sharp change from daytime to nighttime chemistry as depicted in Fig. 2a for Finokalia station (Fig. 2a). During the eclipse period hydroxyl ( $OH$ ) and hydrogen peroxy ( $HO_2$ ) radicals, mainly photochemically produced, show rapid decrease

## Eclipse effects on surface atmospheric photooxidants

P. Zanis et al.

Title Page

Abstract

Introduction

Conclusions

References

Tables

Figures

◀

▶

◀

▶

Back

Close

Full Screen / Esc

Printer-friendly Version

Interactive Discussion

by more than an order of magnitude to nighttime levels. Simultaneously nitrate ( $\text{NO}_3$ ) radical – mainly present during night – is increasing to the pptv level typical of nighttime conditions over the area (Vrekoussis et al., 2006, 2007). Similar conclusions are drawn for the other observational sites like Kastelorizo where  $\text{NO}_3$  radicals reach 4 pptv during the eclipse maximum when OH and  $\text{HO}_2$  radicals decrease by two orders of magnitude.

This drastic and sudden change from daytime to nighttime chemistry during the eclipse has also markedly affected the modelled  $\text{O}_3$  budget changes simulated by the chemical box model for Finokalia (location with 95.6% coverage). Indeed, comparing simulations both by considering and by neglecting the perturbation of photodissociation rates due to the solar eclipse, it was calculated a mean decrease in the net ozone production rate ( $\text{NetPO}_3 = \text{PO}_3 - \text{QO}_3$ ) of 0.86 ppbv/h when integrated over the eclipse period (09:30–12:00; Fig. 3b) with much higher rates up to 1.60 ppbv/h around the maximum sun coverage. The  $\text{O}_3$  production term ( $\text{PO}_3$ ) was calculated from the conversion rate of NO to  $\text{NO}_2$  by  $\text{RO}_2$  radicals while the  $\text{O}_3$  loss term ( $\text{QO}_3$ ) was derived from the rate of the  $\text{O}^1\text{D}$  reaction with  $\text{H}_2\text{O}$  and of  $\text{O}_3$  reactions with  $\text{HO}_x$  and with unsaturated hydrocarbons. A higher change in  $\text{NetPO}_3$  of 1.36 ppbv/h was calculated by the box model for Kastelorizo (location with almost 100% coverage) averaged between the time window 09:30 and 12:00 UTC, and maximizes at about 2.9 ppbv/h during the maximum sun coverage. In parallel  $\text{NO}_2$  increases due to the absence of  $\text{NO}_2$  photodissociation as indicated by the observed almost zero  $\text{JNO}_2$  values.

### 3.3 Regional air quality model results

As described in Sect. 2.3 CAMx calculated the diurnal variation of the photolysis rate  $\text{JNO}_2$  for eclipse and no-eclipse conditions. An example for these calculations is shown in Fig. 4.  $\text{NO}_2$  photolysis rates (black curve) follow a sinusoidal curve increasing gradually after 04:00 UTC and returning to almost zero values after around 16:30 UTC. When considering the eclipse in the calculations (magenta curve), the modelled  $\text{NO}_2$  photolysis rates gradually decrease after 09:30 UTC to minimize at around 11:00 UTC and one hour later return to the non-eclipse values. It should be noted the good level

## Eclipse effects on surface atmospheric photooxidants

P. Zanis et al.

Title Page

Abstract

Introduction

Conclusions

References

Tables

Figures

◀

▶

◀

▶

Back

Close

Full Screen / Esc

Printer-friendly Version

Interactive Discussion

of agreement at Finokalia between the modelled  $\text{JNO}_2$  values (Fig. 4a) and the observed  $\text{JNO}_2$  values (Fig. 2a). The maximum of the observed  $\text{JNO}_2$  values is around  $8.1 \times 10^{-3} \text{ s}^{-1}$  while the respective value calculated in CAMx is  $7.6 \times 10^{-3} \text{ s}^{-1}$ . Furthermore the appearance of clouds just after the eclipse introduced large variability in the observed  $\text{JNO}_2$  and  $\text{JO}^1\text{D}$  signals (Fig. 2a) while similarly the impact of clouds on modelled photolysis rates is also evident after 13:00 UTC at the site of Finokalia (Fig. 4a). Note that the relative reduction of photolysis rates is space dependent. To depict the impact of eclipse on  $\text{JNO}_2$  over the whole modelling region, the percentage of  $\text{JNO}_2$  relative decrease  $(\text{JNO}_{2_{ecl}} - \text{JNO}_{2_o}) / \text{JNO}_{2_o}$  was plotted over the master domain (here subscript “o” denoting simulations without eclipse and “ecl” simulation with eclipse) averaged for the time window 10:00–11:00 UTC (Fig. 5). A decrease in  $\text{JNO}_2$  of 60–65% was calculated for Kastelorizo and 55–60% for Finokalia, 45–50% for Pallini (Athens) and 40–45% for the Thessaloniki.

The values of  $\text{O}_3$ ,  $\text{NO}_2$  and  $\text{NO}$  simulated by CAMx and averaged over the time window 09:30–12:00 UTC when the eclipse took place for the four different sites are shown in Table 2. Comparing the simulations (Table 2) with the observations (Table 1) the following remarks can be made:

1. The simulated  $\text{O}_3$  at Kastelorizo is significantly lower than the observations. Similarly the simulated  $\text{NO}_x$  levels are underestimated compared to the observations, possibly due to generally underestimated anthropogenic emissions over Turkey, which lies only a few kilometers away from Kastelorizo and/or to the clean-atmosphere boundaries that was assumed for this run: Kastelorizo is the easternmost Greek island close to the edges of our domain.
2. At Finokalia both the simulated  $\text{O}_3$  and  $\text{NO}_x$  values agree with the observations.
3. The modelled  $\text{O}_3$ ,  $\text{NO}_2$  and  $\text{NO}$  values at Pallini and Thessaloniki compare rather well with the respective observations.
4. Both the observed and modelled  $\text{O}_3$  levels at Pallini are lower than at Thessaloniki

## Eclipse effects on surface atmospheric photooxidants

P. Zanis et al.

Title Page

Abstract

Introduction

Conclusions

References

Tables

Figures

◀

▶

◀

▶

Back

Close

Full Screen / Esc

Printer-friendly Version

Interactive Discussion

**Eclipse effects on surface atmospheric photooxidants**

P. Zanis et al.

Title Page

Abstract

Introduction

Conclusions

References

Tables

Figures

◀

▶

◀

▶

Back

Close

Full Screen / Esc

Printer-friendly Version

Interactive Discussion

by a few ppbv whereas both the observed and modelled NO<sub>x</sub> levels at Pallini are slightly higher than at Thessaloniki. This pattern is coherent with the non-linear behaviour in O<sub>3</sub> production that associates an increase in NO<sub>x</sub> in these highly polluted sites with a suppression of O<sub>3</sub> production.

5 The average differences of O<sub>3</sub>, NO<sub>2</sub> and NO between eclipse and non-eclipse conditions in CAMx simulations over the time window of the eclipse (09:30–12:00 UTC) and for maximum coverage of the sun-disk for the four sites are indicated in Table 3. At the relatively unpolluted sites of Kastelorizo and Finokalia, the CAMx simulations indicate an ozone decrease of only –0.4 ppbv for Kastelorizo and –1.0 ppbv for Finokalia at the  
 10 time of the maximum coverage of the sun-disk. These values are smaller than the standard deviation of the ozone measurements during the time window of the eclipse for both sites (see Table 1). Specifically the standard deviation of the ozone measurements for the time window 09:30–12:00 is 4.3 ppbv at Kastelorizo and 2.5 ppbv at Finokalia. If we also consider that the ozone instruments have a detection limit of about 1 ppbv  
 15 then it is easily conceived why a clear evidence of the solar eclipse on O<sub>3</sub> cannot be supported for both Kastelorizo and Finokalia (Fig. 1). Similarly the CAMx simulations indicate only small changes for NO and NO<sub>2</sub> for Kastelorizo and Finokalia during the solar eclipse. In particular, increases in NO<sub>2</sub> of 0.06 and 0.11 ppbv and decreases in NO of 0.03 and 0.05 ppbv have been calculated at the time of the maximum coverage of sun-disk for Kastelorizo and Finokalia, respectively. It should be further noted  
 20 from Table 3 that the differences from the observations of O<sub>3</sub>, NO<sub>2</sub> and NO between their averaged values in the time window of maximum total solar obscuration (10:30–11:00 UTC) and their averaged values from both the time windows before and after the eclipse (09:30–10:00 UTC and 11:30–12:00 UTC) are generally not consistent with the  
 25 CAMx calculations of the eclipse effects on these species. This inconsistency points to the fact that at these relatively unpolluted sites the eclipse effects on the observations of O<sub>3</sub>, NO<sub>2</sub> and NO are masked.

Mind also that the changes in O<sub>3</sub>, NO<sub>2</sub> and NO between eclipse and non-eclipse conditions in the CAMx simulations for Kastelorizo are smaller than for Finokalia even

though at Kastelorizo there was almost 100% sun coverage. This discrepancy can be attributed to the lower pollution levels at Kastelorizo in CAMx runs. Hence we anticipate that the CAMx simulations of the changes in  $O_3$ ,  $NO_2$  and NO between eclipse and non-eclipse conditions for Kastelorizo are underestimated because of the underestimation of  $O_3$  and NOx levels in the CAMx results compared to observations (see Tables 1 and 2), earlier discussed.

At the polluted sites the CAMx simulations indicate an ozone decrease of 6.4 ppbv for Pallini and 10.6 ppbv for Thessaloniki at the time of the maximum coverage of the sun-disk. The CAMx simulated  $O_3$  change between eclipse and non-eclipse conditions integrated over the time window of the eclipse 09:30–12:00 UTC is  $-4.1$  ppbv for Pallini and  $-5.8$  ppbv for Thessaloniki (see also Table 3). These simulated ozone decreases due to the solar eclipse are in good agreement with the in-situ ozone observations at the two polluted sites (see Table 3). For example, the difference in the observed  $O_3$  between the averaged value in the time window of maximum total solar obscuration (10:30–11:00 UTC) and the averaged values from both the time windows before and after the eclipse (09:30–10:00 UTC and 11:30–12:00 UTC) is  $-8$  and  $-4$  ppbv for Thessaloniki and Pallini, respectively.

Furthermore, CAMx simulations indicate a decrease in NO of  $-2.55$  ppbv and an increase in  $NO_2$  of 3.41 ppbv for Pallini over the time window of the eclipse 09:30–12:00 UTC. The observations of NO and  $NO_2$  at Pallini taking the difference between the time window of the maximum coverage of the sun disk and the time windows before and after the completion of the solar eclipse indicate a NO decrease of  $-2.1$  ppbv and  $NO_2$  increase of 5.6 ppbv. The CAMx simulations at Thessaloniki indicate a decrease in NO of  $-0.19$  ppbv and an increase in  $NO_2$  of 3.44 ppbv over the time window of the eclipse 09:30–12:00 UTC whereas the observations indicate NO decrease of about  $-1$  ppbv and  $NO_2$  increase of about 2 ppbv. Hence the CAMx simulated values of the differences of  $O_3$ ,  $NO_2$  and NO between eclipse and non-eclipse conditions compare reasonably well with observations for both Pallini and Thessaloniki.

The eclipse effect over Greece as calculated by CAMx is depicted in Fig. 6 that

## Eclipse effects on surface atmospheric photooxidants

P. Zanis et al.

Title Page

Abstract

Introduction

Conclusions

References

Tables

Figures

◀

▶

◀

▶

Back

Close

Full Screen / Esc

Printer-friendly Version

Interactive Discussion

shows the differences in  $\text{NO}_2$ ,  $\text{NO}$  and  $\text{O}_3$  between eclipse and non-eclipse conditions for the first model level Z1 (<22 m) averaged over the time window 10:00–11:00 UTC. Over Greece the maximum impacts of the eclipse on  $\text{O}_3$ ,  $\text{NO}_2$  and  $\text{NO}$  are calculated to occur over the large urban agglomerations of Athens, and Thessaloniki where the maximum of the emissions occur. Furthermore, we note a stripe at the western Aegean See with notable eclipse effects on these air pollutants which might be associated to ship emissions since ship trails coincide in space.

Comparing the net  $\text{O}_3$  production calculated by the box model and by the regional air-quality model (see Table 4) there is agreement in the calculated  $\text{NetPO}_3$  and the  $\text{NetPO}_3$  due to eclipse ( $\Delta\text{NetPO}_3$ ) when integrated over the eclipse window at Finokalia. As explained the box model is evaluating the effect of eclipse on  $\text{O}_3$  production resulting from the photolysis rates changes alone. Thus it is calculating higher changes close to the maximum sun coverage than the regional model that, in addition, accounts for air masses mixing due to transport. However, at Kastelorizo the comparison between box-model and CAMx calculations of  $\text{NetPO}_3$  and  $\Delta\text{NetPO}_3$  is not satisfactory with providing lower estimates in all cases (Table 4). The box model simulations that are forced to reproduce observed  $\text{NO}_x$  levels indicate indeed larger impact of the eclipse on  $\text{NetPO}_3$  at Kastelorizo than at Finokalia. As earlier discussed this underestimation could be attributed to generally underestimated anthropogenic emissions over Turkey and/or to clean-atmosphere boundaries conditions assumed for the CAMx run at the edge of our domain where the Kastelorizo is located.

#### 4 Summary and conclusions

The present work investigated the chemical effects of the solar eclipse of 29 March 2006 on surface air quality levels over Greece based on observations at a number of sites in conjunction with chemical box modelling and 3-D air-quality modelling. Emphasis has been given on surface ozone and other photooxidants at four Greek sites Kastelorizo, Finokalia (Crete), Pallini (Athens) and Thessaloniki, which are located at

### Eclipse effects on surface atmospheric photooxidants

P. Zanis et al.

Title Page

Abstract

Introduction

Conclusions

References

Tables

Figures

⏪

⏩

◀

▶

Back

Close

Full Screen / Esc

Printer-friendly Version

Interactive Discussion

gradually increasing distances from the eclipse path and are characterized by different air pollution levels. The different solar obscuration at each site combined with a variety of environments, by means of air quality level, namely polluted urban/suburban (Thessaloniki, Pallini), and relatively unpolluted coastal (Finokalia, Kastelorizo) enabled a thorough investigation of the response of photochemistry to an abrupt photolytical change.

At the relatively unpolluted sites of Kastelorizo and Finokalia no clear impact of solar eclipse on surface  $O_3$ ,  $NO_2$  and  $NO$  concentrations can be deduced from the observations and model simulations. The observations corroborate with chemical box modelling and 3-D air-quality modelling.  $O_3$  at Finokalia has been associated with a mean decrease in the net ozone production rate of 0.86 ppbv/h (box model) and 0.60 ppbv/h (CAMx) when integrated over the eclipse period (09:30–12:00 UTC). Similarly, at Kastelorizo (location with almost 100% coverage)  $O_3$  has been associated with a mean decrease in the net ozone production rate of 1.36 ppbv/h (box model) and 0.16 ppbv/h (CAMx). Such changes in the net ozone production between eclipse and non eclipse conditions, as calculated by both box and 3-D air quality models, are rather small compared to the ozone variability and hence the solar eclipse effects on ozone can be easily masked by transport.

Box model calculations also demonstrated the rapid decrease of the photochemically produced  $OH$  and  $HO_2$  radicals by more than an order of magnitude to nighttime levels at Finokalia during the eclipse period. Simultaneously the  $NO_3$  radical concentration, the main nighttime oxidant species, increased to the pptv level, which is typical for nighttime conditions over the area.

At the polluted urban and suburban sites of Thessaloniki and Pallini, respectively, solar eclipse effects on  $O_3$ ,  $NO_2$  and  $NO$  concentrations are clearly indicated from both the measurements and 3-D air-quality modelling. The net effect is a decrease in  $O_3$  and  $NO$  while  $NO_2$  is accumulated. The common behaviour of  $O_3$ ,  $NO_2$  and  $NO$  concentrations at the two polluted sites, Pallini and Thessaloniki, can be attributed to their perturbation from the photostationary state of  $O_3$ ,  $NO$  and  $NO_2$  during the

## Eclipse effects on surface atmospheric photooxidants

P. Zanis et al.

Title Page

Abstract

Introduction

Conclusions

References

Tables

Figures

◀

▶

◀

▶

Back

Close

Full Screen / Esc

Printer-friendly Version

Interactive Discussion

eclipse, with  $\text{NO}_2$  formed from the reaction of  $\text{O}_3$  with  $\text{NO}$  while at the same time  $\text{NO}_2$  is not efficiently photolysed. The 3-D air quality modelling over Greece simulates the maximum effects of the eclipse on  $\text{O}_3$ ,  $\text{NO}_2$  and  $\text{NO}$  at the large urban agglomerations of Athens, and Thessaloniki where the maximum of the emissions occur.

5 The net  $\text{O}_3$  production ( $\text{NetPO}_3$ ) and the impact of changing photolysis rates on it ( $\Delta\text{NetPO}_3$ ) calculated by the box model and by the regional air-quality model agree reasonably well when integrated over the eclipse window at Finokalia but is underestimated by CAMx for Kastelorizo. This underestimation is linked to an underestimation of CAMx  $\text{O}_3$ , and  $\text{NO}_x$  levels which could be in turn due to generally underestimated anthropogenic emissions over Turkey and/or the fact that Kastelorizo is close to the edge  
10 of our domain with clean-atmosphere boundaries conditions assumed for the CAMx run.

*Acknowledgements.* Compilation and presentation of this work has been facilitated by the AC-CENT – EU network of excellence. Support by a research and education PYTHAGORAS  
15 II grant co-funded by the Greek Ministry of Education (25%) and the European Social Fund (75%) is acknowledged. The air quality and meteorological data of Pallini, Athens were kindly provided by the Air Quality Monitoring Network of Athens International Airport (AIA) Eleftherios Venizelos.

## References

- 20 CAMx User's Guide, Version 4.30, ENVIRON International Corporation, February 2006, <http://www.camx.com>, 2006.
- Curtis, A. R. and Sweetenham, W. P.: FACSIMILE/CHEKMAT User's Manual AERE R-12805, United Kingdom Atomic Energy Authority (UKAEA), Harwell, 1988.
- Gerasopoulos, E., Kouvarakis, G., Vrekoussis, M., Kanakidou, M., and Mihalopoulos, N.:  
25 Ozone variability in the marine boundary layer of the eastern Mediterranean based on 7-year observations, *J. Geophys. Res.*, 110(D15), D15309, doi:10.1029/2005JD005991, 2005.
- Gerasopoulos, E., Kouvarakis, G., Vrekoussis, M., Donoussis, C., Mihalopoulos, M., and

---

## Eclipse effects on surface atmospheric photooxidants

P. Zanis et al.

---

Title Page

Abstract

Introduction

Conclusions

References

Tables

Figures

◀

▶

◀

▶

Back

Close

Full Screen / Esc

Printer-friendly Version

Interactive Discussion

- Kanakidou, M.: Photochemical ozone production in the Eastern Mediterranean, *Atmos. Environ.*, 40(17), 3057–3069, 2006.
- Fabian, P., Rappenglueck, B., Stohl, A., Werner, H., Winterhalter, M., Schlager, H., Stock, P., Berresheim, H., Kaminski, U., Koepke, P., Reuder, J., and Birmili, W.: Boundary layer photochemistry during a total solar eclipse, *Meteorologische Zeitschrift*, 10(3), 187–192, 2001.
- Founda, D., Melas, D., Lykoudis, S., Lisaridis, I., Gerasopoulos, E., Kouvarakis, G., Petrakis, M., and Zerefos, C.: The effect of the total solar eclipse of March 29, 2006 on meteorological variables in Greece, *Atmos. Chem. Phys. Discuss.*, 7, 10 631–10 667, 2007.
- Poupkou, A., Symeonidis, P., Lisaridis, I., Pouspourika, E., Yay, O.D., Melas, D., Ziomas, I., Balis, D., and Zerefos, C.: Compilation of an emission inventory for the purpose of studying the regional photochemical pollution in the Balkan Region, *Proceedings of the Quadrennial Ozone Symposium 2004*, Kos, Greece, 902–903, 2004.
- Madronich, S.: UV radiation in the natural and perturbed atmosphere, in: *Environmental Effects of UV (Ultraviolet) Radiation*, edited by: Tevini, M., Lewis Publisher, Boca Raton, 17–69, 1993.
- Mavrakis, A., Theoharatos, G., and Lykoudis, S.: Ultraviolet radiation and surface ozone variations during the solar eclipse of 11 Aug. 1999, over Attica, Greece, *Proceeding of the XX Quadrennial Ozone Symposium*, Vol. II, Session 6, 1126–1127, 2004.
- Mihalopoulos, N., Stephanou, E., Kanakidou, M., Pilitsidis, S., and Bousquet, P.: Tropospheric aerosol ionic composition above the Eastern Mediterranean Area, *Tellus*, 49B, 314–326, 1997.
- Sciare J., Kanakidou M., and Mihalopoulos, N.: Diurnal and seasonal variation of atmospheric dimethyl sulfoxide (DMSO) at Amsterdam island in the southern Indian Ocean, *J. Geophys. Res.*, 105, 17 257–17 265, 2000.
- Srivastava, G. P., Pakkiri, M. P. M., and Balwalli, R. R.: Ozone concentration measurements near the ground at Raichur during the solar eclipse of 1980. *Proceedings of Indian Natural Sciences Academy*, A48(3), 138–142, 1982.
- Tsigaridis, K. and Kanakidou, M.: Importance of Volatile Organic Compounds Photochemistry Over a Forested Area in Central Greece, *Atmos. Environ.*, 36(19), 3137–3146, 2002.
- Vrekoussis, M., Kanakidou, M., Mihalopoulos, N., Crutzen, P. J., Lelieveld, J., Perner, D., Berresheim, H., and Baboukas, E.: Role of the NO<sub>3</sub> radicals in oxidation processes in the eastern Mediterranean troposphere during the MINOS campaign, *Atmos. Chem. Phys.*, 4,

---

**Eclipse effects on surface atmospheric photooxidants**P. Zanis et al.

---

[Title Page](#)[Abstract](#)[Introduction](#)[Conclusions](#)[References](#)[Tables](#)[Figures](#)[◀](#)[▶](#)[◀](#)[▶](#)[Back](#)[Close](#)[Full Screen / Esc](#)[Printer-friendly Version](#)[Interactive Discussion](#)

169–182, 2004,

<http://www.atmos-chem-phys.net/4/169/2004/>.

Vrekoussis, M., Liakakou, E., Mihalopoulos, N., Kanakidou, M., Crutzen, P. J., and Lelieveld, J.: Formation of  $\text{HNO}_3$  and  $\text{NO}_3^-$  in the anthropogenically-influenced eastern Mediterranean marine boundary layer, *Geophys. Res. Lett.*, 33, L05811, doi:10.1029/2005GL025069, 2006.

Vrekoussis, M., Mihalopoulos, N., Gerasopoulos, E., Kanakidou, M., Crutzen, P. J., and Lelieveld, J.: Two-years of  $\text{NO}_3$  radical observations in the boundary layer over the Eastern Mediterranean, *Atmos. Chem. Phys.*, 7, 315–327, 2007

Zanis, P., Zerefos, C. S., Gilge, S., Melas, D., Balis, D., Ziomas, I., Gerasopoulos, E., Tzoumaka, P., Kaminski, U., and Fricke, W.: Comparison of measured and modelled surface ozone concentrations at two different sites in Europe during the solar eclipse on August 11, 1999, *Atmos. Environ.*, 35, 4663–4673, 2001.

Zerefos, C. S., Balis, D. S., Zanis, P., Meleti, C., Bais, A. F. Tourpali, K., Melas, D., Ziomas, I., Galani, E., Kourtidis, K., Papayannis, A., and Gogosheva, Z.: Changes in surface UV solar irradiance and ozone over the Balkans during the eclipse of August 11, 1999, *Adv. Space Res.*, 27(12), 1955–1963, 2001.

Zerefos, C. S., Balis, D. S., Meleti, C., Bais, A. F., Tourpali, K., Vanicek, K., Cappelani, F., Kaminski, U., Tiziano, C., Stubi, R., Formenti, P., and Andreae, A.: Changes in environmental parameters during the solar eclipse of August 11, 1999, over Europe. Effects on surface UV solar irradiance and total ozone, *J. Geophys. Res.*, 105(D21), 26 463–26 473, 2000.

ACPD

7, 11399–11428, 2007

## Eclipse effects on surface atmospheric photooxidants

P. Zanis et al.

Title Page

Abstract

Introduction

Conclusions

References

Tables

Figures

◀

▶

◀

▶

Back

Close

Full Screen / Esc

Printer-friendly Version

Interactive Discussion

**Eclipse effects on  
surface atmospheric  
photooxidants**

P. Zanis et al.

**Table 1.** Observations of O<sub>3</sub>, NO<sub>2</sub> and NO averaged over the time window 09:30–12:00 UTC when the eclipse took place for the sites Kastelorizo, Finokalia, Pallini and Thessaloniki. The standard deviation is given in parenthesis.

	O <sub>3</sub> (ppbv)	NO <sub>2</sub> (ppbv)	NO (ppbv)
Kastelorizo	68.6 (±4.3)	1.57 (±1.40)	0.39 (±0.28)
Finokalia	42.7 (±2.5)	0.34 (±0.13)	0.07 (±0.02)
Pallini, Athens	36.9 (±3.6)	15.59 (±3.42)	4.83 (±1.13)
Thessaloniki	43.5 (±4.3)	12.11 (±2.69)	1.89 (±1.16)

[Title Page](#)[Abstract](#)[Introduction](#)[Conclusions](#)[References](#)[Tables](#)[Figures](#)[I◀](#)[▶I](#)[◀](#)[▶](#)[Back](#)[Close](#)[Full Screen / Esc](#)[Printer-friendly Version](#)[Interactive Discussion](#)

## Eclipse effects on surface atmospheric photooxidants

P. Zanis et al.

**Table 2.** Simulations of O<sub>3</sub>, NO<sub>2</sub> and NO by CAMx averaged over the time window 09:30–12:00 UTC when the eclipse took place for the sites Kastelorizo, Finokalia, Pallini and Thessaloniki. The standard deviation is given in parenthesis.

	O <sub>3</sub> (ppbv)	NO <sub>2</sub> (ppbv)	NO (ppbv)
Kastelorizo	51.7 (±0.6)	0.17 (±0.01)	0.02 (±0.01)
Finokalia	43.5 (±0.6)	0.30 (±0.04)	0.05 (±0.02)
Pallini, Athens	34.8 (±6.4)	19.03 (±7.30)	6.21 (±4.28)
Thessaloniki	42.48 (±3.4)	11.75 (±2.80)	3.22 (±0.50)

Title Page

Abstract

Introduction

Conclusions

References

Tables

Figures

⏪

⏩

◀

▶

Back

Close

Full Screen / Esc

Printer-friendly Version

Interactive Discussion

## Eclipse effects on surface atmospheric photooxidants

P. Zanis et al.

**Table 3.** Differences of O<sub>3</sub>, NO<sub>2</sub> and NO between eclipse and non-eclipse conditions in CAMx simulations over the time window of the eclipse 09:30–12:00 UTC for the sites Kastelorizo, Finokalia, Pallini and Thessaloniki. The values in parentheses correspond to the respective values of differences for the maximum sun coverage. The differences from the observations of O<sub>3</sub>, NO<sub>2</sub> and NO between their averaged values in the time window of maximum total solar obscuration 10:30–11:00 UTC and their averaged values from both the time windows before and after the eclipse (09:30–10:00 UTC and 11:30–12:00 UTC) are also provided for comparison.

	$\Delta\text{O}_3$ (ppbv) Model	Obs	$\Delta\text{NO}_2$ (ppbv) Model	Obs	$\Delta\text{NO}$ (ppbv) Model	Obs
Kastelorizo	−0.3 (−0.4)	0.8	0.03 (0.06)	−0.35	−0.01 (−0.03)	−0.06
Finokalia	−0.7 (−1.0)	2.3	0.06 (0.11)	−0.07	−0.02 (−0.05)	0.00
Pallini, Athens	−4.1 (−6.4)	−4.0	3.41 (5.75)	5.56	−2.35 (−4.99)	−2.10
Thessaloniki	−5.8 (−10.6)	−8.4	3.44 (7.3)	1.84	−0.19 (−1.25)	−0.93

Title Page

Abstract

Introduction

Conclusions

References

Tables

Figures

⏪

⏩

◀

▶

Back

Close

Full Screen / Esc

Printer-friendly Version

Interactive Discussion

## Eclipse effects on surface atmospheric photooxidants

P. Zanis et al.

**Table 4.** Net O<sub>3</sub> chemical production (NetPO<sub>3</sub>=PO<sub>3</sub>-QO<sub>3</sub>) at the four studied stites for eclipse and non-eclipse conditions over the time window of eclipse 09:30–12:00 UTC in CAMx and Box Model as well as their difference ΔNetPO<sub>3</sub> between eclipse and non-eclipse conditions.

	NetPO <sub>3</sub> eclipse (ppbv/h)	NetPO <sub>3</sub> non- eclipse (ppbv/h)	ΔNetPO <sub>3</sub> (ppbv/h)
Kastelorizo			
CAMx	0.17	0.33	−0.16
Box Model	1.10	2.46	−1.36
Finokalia			
CAMx	0.72	1.32	−0.60
Box Model	0.55	1.41	−0.86

Title Page

Abstract

Introduction

Conclusions

References

Tables

Figures

◀

▶

◀

▶

Back

Close

Full Screen / Esc

Printer-friendly Version

Interactive Discussion

## Eclipse effects on surface atmospheric photooxidants

P. Zanis et al.

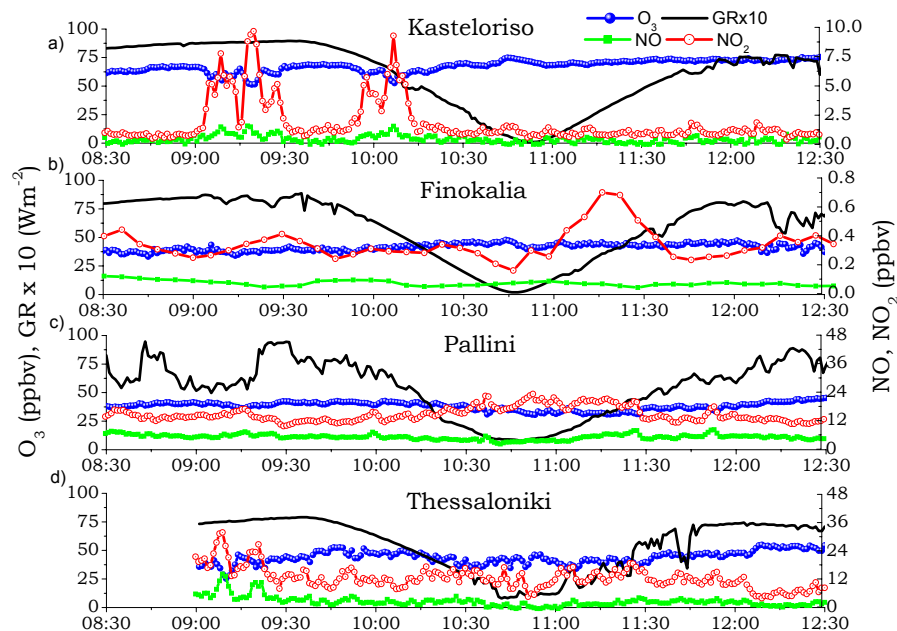


**Fig. 1.** Time series of  $O_3$ ,  $NO$ ,  $NO_2$  and global radiation at Kastelorizo, Finokalia, Pallini and Thessaloniki during the eclipse day of 29 March 2006 from 08:38 to 12:28. Time is expressed in UTC.

Title Page

Abstract

Introduction

Conclusions

References

Tables

Figures

◀

▶

◀

▶

Back

Close

Full Screen / Esc

Printer-friendly Version

Interactive Discussion

## Eclipse effects on surface atmospheric photooxidants

P. Zanis et al.

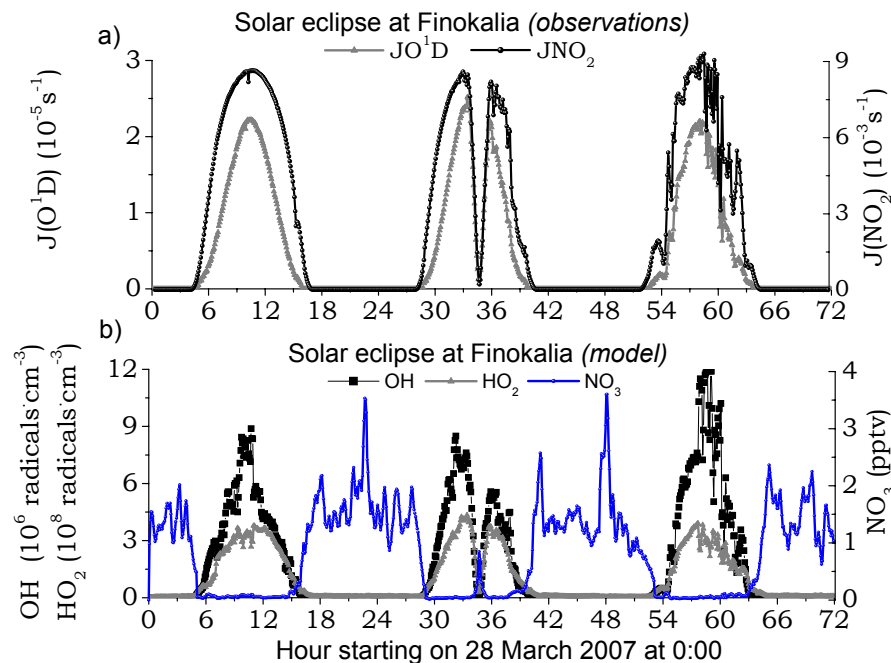


**Fig. 2.** (a) Measured photolysis rates of  $NO_2$  ( $JNO_2$ ) and  $O_3$  ( $JO^1D$ ) at Finokalia over a 3 days period around the eclipse of the 29 March 2006. (b) hydroxyl ( $OH$ ), hydrogen peroxy ( $HO_2$ ) and nitrate ( $NO_3$ ) radical levels simulated by the chemical box model for Finokalia during these 3 days. Time is expressed in UTC.

[Title Page](#)[Abstract](#)[Introduction](#)[Conclusions](#)[References](#)[Tables](#)[Figures](#)[◀](#)[▶](#)[◀](#)[▶](#)[Back](#)[Close](#)[Full Screen / Esc](#)[Printer-friendly Version](#)[Interactive Discussion](#)

## Eclipse effects on surface atmospheric photooxidants

P. Zanis et al.

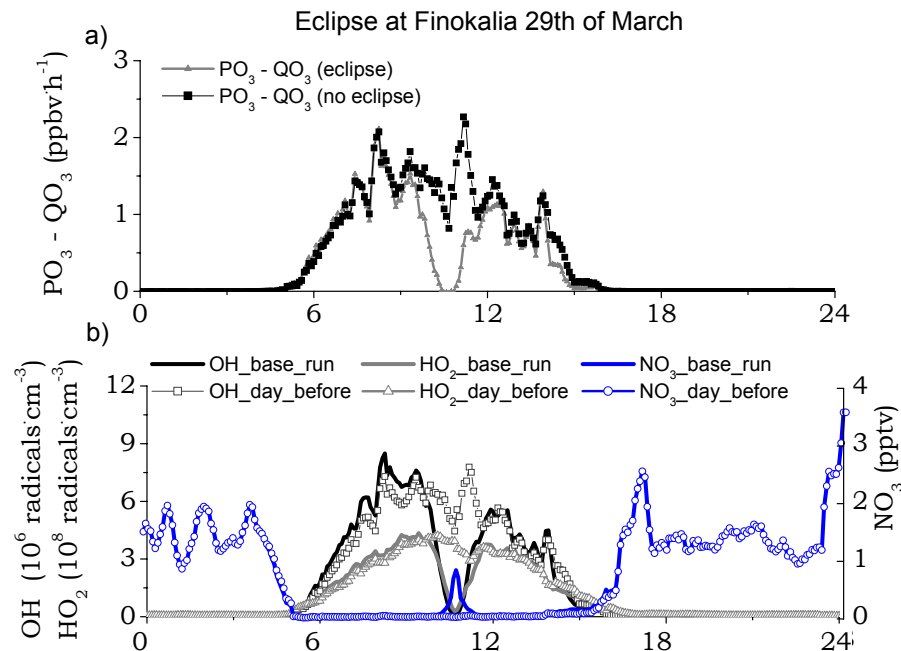


**Fig. 3.** (a) Net O<sub>3</sub> chemical production (NetPO<sub>3</sub>=PO<sub>3</sub>-QO<sub>3</sub>) at Finokalia during the day of the eclipse, 29 March 2006, simulated by considering the effect of eclipse of photolysis rates (NetPO<sub>3</sub>\_base-run) and by neglecting it (NetPO<sub>3</sub>\_ydaybefore) (b) as (a) but for OH, HO<sub>2</sub> and NO<sub>3</sub> radical levels. Time is expressed in UTC. NetPO<sub>3</sub>= PO<sub>3</sub> -QO<sub>3</sub>, where PO<sub>3</sub>=ΣR<sub>RO2NO</sub>NO, QO<sub>3</sub>=O<sup>1</sup>D+ H<sub>2</sub>O, alkenes + O<sub>3</sub>.

Title Page

Abstract

Introduction

Conclusions

References

Tables

Figures

◀

▶

◀

▶

Back

Close

Full Screen / Esc

Printer-friendly Version

Interactive Discussion

Eclipse effects on  
surface atmospheric  
photooxidants

P. Zanis et al.

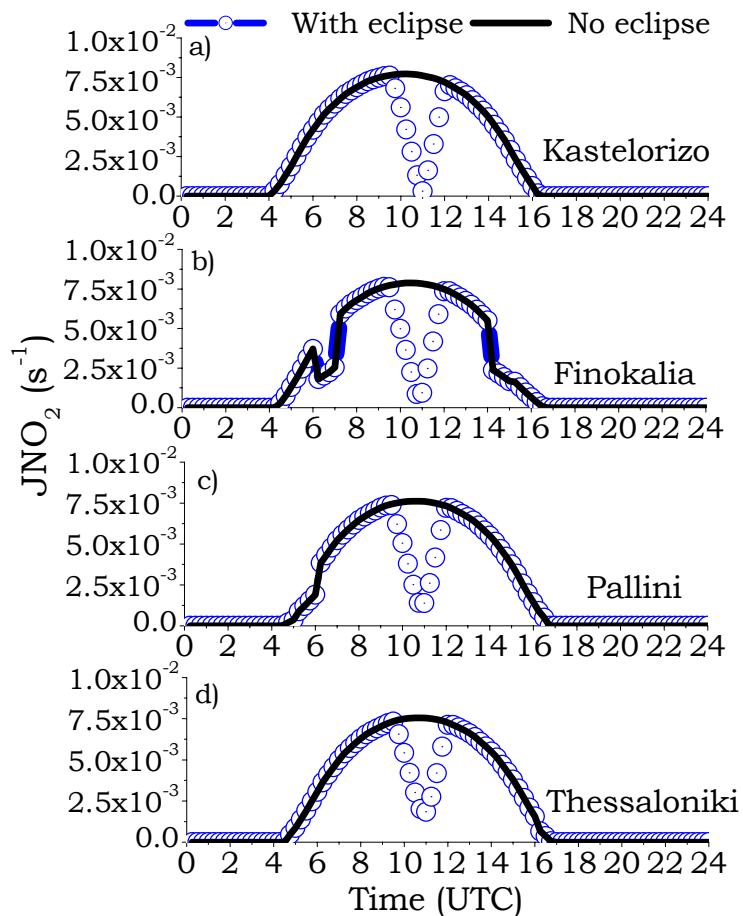


**Fig. 4.** Diurnal variation of the photolysis rate constant  $J(\text{NO}_2)$  values calculated in CAMx simulations for eclipse and non-eclipse conditions at Kastelorizo, Finokalia, Pallini and Thessaloniki.

[Title Page](#)[Abstract](#)[Introduction](#)[Conclusions](#)[References](#)[Tables](#)[Figures](#)[◀](#)[▶](#)[◀](#)[▶](#)[Back](#)[Close](#)[Full Screen / Esc](#)[Printer-friendly Version](#)[Interactive Discussion](#)

Eclipse effects on  
surface atmospheric  
photooxidants

P. Zanis et al.

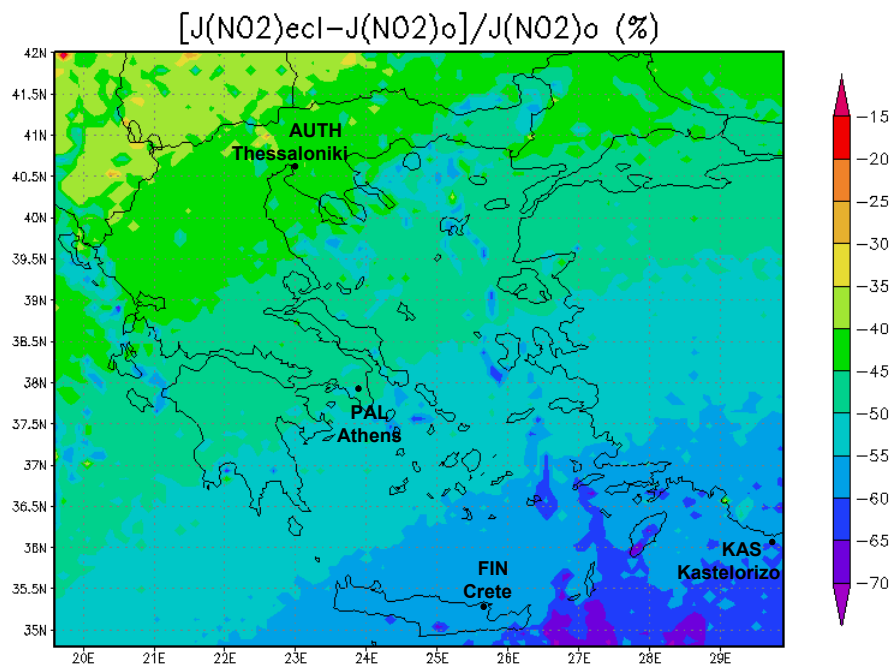


**Fig. 5.** Percentage decrease of  $\text{NO}_2$  photolysis rates averaged for the time window 10:00–11:00 UTC over the master modeling domain. The four dots show the four observational sites.

Title Page

Abstract

Introduction

Conclusions

References

Tables

Figures

◀

▶

◀

▶

Back

Close

Full Screen / Esc

Printer-friendly Version

Interactive Discussion

## Eclipse effects on surface atmospheric photooxidants

P. Zanis et al.

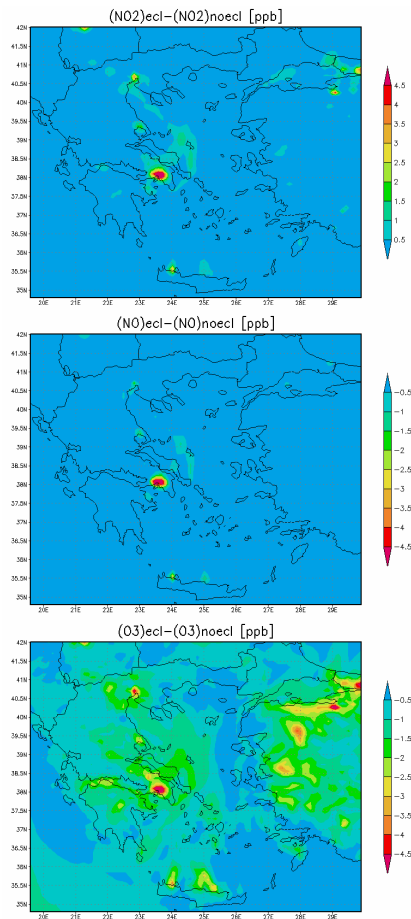


**Fig. 6.** Differences of (a) NO<sub>2</sub>, (b) NO and (c) O<sub>3</sub> between eclipse and non-eclipse conditions in CAMx simulations over the master modeling domain for the first model level Z1 (<22 m) averaged for the time window 10:00–11:00 UTC.

[Title Page](#)[Abstract](#)[Introduction](#)[Conclusions](#)[References](#)[Tables](#)[Figures](#)[◀](#)[▶](#)[◀](#)[▶](#)[Back](#)[Close](#)[Full Screen / Esc](#)[Printer-friendly Version](#)[Interactive Discussion](#)